8. Hermanek P, Sobin L. TNM classification of malignant tumors. Fourth ed. Berlin: Springer-Verlag;1987.
9. Ohtsu A, Boku N, Muro K, *et al.* Definitive chemoradiotherapy for T4 and/or M1 lymph node squamous cell carcinoma of the esophagus. *J Clin Oncol* 1999;17:2915–2921.
10. Miyazaki S, Satomi S. Definitive chemoradiotherapy and salvage esophagectomy for squamous cell carcinoma of the esophagus [In Japanese]. *Nippon Geka Gakkai Zasshi* 2004;105:485–488.
11. Aaronson NK, Ahmedzai S, Bergman B, *et al.* The European Organization for Research and Treatment of Cancer QLQ-C30: A quality-of-life instrument for use in international clinical trials in oncology. *J Natl Cancer Inst* 1993;85:365–376.
12. Wilson KS, Lim JT. Primary chemo-radiotherapy and selective oesophagectomy for oesophageal cancer: Goal of cure with organ preservation. *Radiother Oncol* 2000;54:129–134.
13. Coia LR, Minsky BD, Berkey BA, *et al.* Outcome of patients receiving radiation for cancer of the esophagus: Results of the 1992-1994 Patterns of Care Study. *J Clin Oncol* 2000;18:455–462.
14. Liao Z, Zhang Z, Jin J, *et al.* Esophagectomy after concurrent chemoradiotherapy improves locoregional control in clinical stage II or III esophageal cancer patients. *Int J Radiat Oncol Biol Phys* 2004;60:1484–1493.
15. Swisher SG, Wynn P, Putnam JB, *et al.* Salvage esophagectomy for recurrent tumors after definitive chemotherapy and radiotherapy. *J Thorac Cardiovasc Surg* 2002;123:175–183.
16. Gardner-Thorpe J, Hardwick RH, Dwerryhouse SJ. Salvage oesophagectomy after local failure of definitive chemoradiotherapy. *Br J Surg* 2007;94:1059–1066.
17. Gebski V, Burmeister B, Smithers BM, *et al.* Survival benefits from neoadjuvant chemoradiotherapy or chemotherapy in oesophageal carcinoma: A meta-analysis. *Lancet Oncol* 2007;8: 226–234.
18. Jingu K, Nemoto K, Kaneta T, *et al.* Temporal change in brain natriuretic Peptide after radiotherapy for thoracic esophageal cancer. *Int J Radiat Oncol Biol Phys* 2007;69:1417–1423.
19. Blazeby JM, Farndon JR, Donovan J, *et al.* A prospective longitudinal study examining the quality of life of patients with esophageal carcinoma. *Cancer* 2000;88:1781–1787.
20. Bonnetain F, Bouche O, Michel P, *et al.* A comparative longitudinal quality of life study using the Spitzer quality of life index in a randomized multicenter phase III trial (FFCD 9102): Chemoradiation followed by surgery compared with chemoradiation alone in locally advanced squamous resectable thoracic esophageal cancer. *Ann Oncol* 2006;17:827–834.

前立腺癌の放射線治療

小川 芳弘
東北大学准教授（放射線腫瘍学分野）

わが国の死亡原因の1位は悪性腫瘍によるもので，高齢者の増加とともにその数は増加しています．前立腺癌患者も年々増加しており，現在年間3万人以上が罹患し，1万人程度が死亡しています[1]．前立腺癌の治療には手術，ホルモン療法，放射線療法などがありますが，近年では侵襲の少ない放射線治療を受ける患者も増加しています．前立腺癌の放射線治療は大きく分けて，外部照射と小線源治療に分かれます．放射線治療を行うにあたっては，その適応を理解し，患者の意思も尊重しながら，適切な照射法を選択することが重要と考えます．

外部照射には，通常の直線加速器によるX線治療とシンクロトロンなどの加速器による陽子線，重粒子線治療とがあります．照射野はリンパ節転移がない場合は前立腺および，病巣の広がりによっては精嚢を含めた照射野とすることが多く，予防的な所属リンパ節の照射はほとんど行われません．放射線の治療効果は前立腺癌のリスク分類によって左右されることが多く，高リスク群では高線量を与えたほうが制御率が高くなることがわかっています[2]．

放射線治療を行う場合，晩期障害は避ける努力をしなければなりません．前立腺癌の放射線治療後の晩期障害には直腸膀胱障害や尿道狭窄，勃起障害などがあり，投与線量が高くなれば，それらの発生頻度は高くなります．高線量を投与する場合は少しでも正常組織の線量を少なくするために，3次元原体照射（3D-CRT; three-dimensional conformal radiotherapy）や強度変調照射（IMRT; intensity modulated radiation therapy）が行われます．特にIMRTは，直腸や尿道の線量を下げるといった，複雑な線量分布を作ることが可能で，高線量投与するためには必要な技術となります．ただし，IMRTを行うためには，技術的，人的要因が大きく，行える施設は限られたものになっています．通常の治療線量は通常分割法の場合（1回2 Gy，週5回照射），低リスク群で70 Gy程度，中リスク群で70～74 Gy程度，高リスク群で74～80 Gy程度となっています．70 Gy以上照射する場合は3D-CRTやIMRTを用いることが推奨されます．わが国は陽子線や重粒子線を用いた治療で世界的にパイオニア的存在となっており，治療成績も良好ですが，まだまだ限られた施設でしか行えず，今後の研究，普及が待たれます．

代表的な治療成績を表に示します[3～7]．放射線治療による晩期障害は通常5%以下という報告が多くなっています．わが国ではホルモン療法を併用することも多くなっていますが，欧米では放射線単独治療の報告が多く，ホルモン療法併用に関しては今後のさらなる検討が必要です．

欧米では20年以上前から前立腺癌に対する小線源治療が行われていましたが，わが国では2003年に厚生労働省から永久刺入患者の退室基準が示され，^{125}Iシード線源による前立腺癌の永久刺入治療が行えるようになりました．現在では全国で数十の施設で治療が行われています．永久刺入治療は治療期間が短いという長所がありますが，その適応はある程度限られたものになります．永久刺入の適応は，アメリカ小線源治療学会（ABS）の基準によると，T1～T2a，Gleasonスコア2～6，PSA＜10 ng/mLであり，肥大した前立腺やTURP後の前立腺に対しては適応外となっています．永久刺入に用いられるシード線源は直径約1 mm，長さ約4.5 mmのチタン製のカプセルで，腰椎麻酔，全身麻酔の下に強砕石位にて60～100本

表　前立腺癌の放射線治療成績 (3D-CRT, IMRT, 粒子線)

報告者 (年)	照射法	患者数 Stage	PSA 値	照射線量 (Gy)	5 年 DSS (%)	5 年 bNED (%)
Hanks GE[3] (USA, 1998)	3D-CRT	*N*=232 T1～T3	PSA<10 ng/mL	<70.0		86
				70.0～71.9		77
				≧72.0		84
			PSA 10～19.9 ng/mL	<71.5	100	29
				71.5～75.8	94	57
				>75.8	100	73
			PSA>20 ng/mL	<71.5	95	8
				71.5～75.8	95	28
				>75.8	96	30
Pollack A[4] (USA, 2002)	3D-CRT	*N*=301 T1～T3		70		64 (6 年)*1
				78		70 (6 年)*1
Zelefsky MJ[5] (USA, 2002)	IMRT	*N*=772				Favorable risk group 92 (3 年)*2
						Intermediate risk group 86 (3 年)*2
						Unfavorable risk group 81 (3 年)*2
ロマリンダ大[6] (USA, 1999)	陽子線	*N*=319 T1～T2b			Overall 97	88
放医研[7] (2005)	炭素線	*N*=201 T1～T3			Overall 89	83
						Low risk group 100
						High risk group 81

DSS: 疾患特異的生存率 (disease-specific survival) bNED: biochemical non-evidence of disease (biochemical disease-free survival)
*1 freedom from failure, *2 PSA relapse-free survival

の線源が刺入されます．治療に要する時間は 1 時間程度で，刺入後 2 日程度で退院可能なことが多くなっています．一方で，わが国では，^{125}I シード線源が使用不可能であった 1990 年代初頭から，^{192}Ir による一時刺入も行われてきました．これは高線量率の組織内照射であり，前立腺部に留置したカテーテルに線源を一時挿入するものです．

局所に限局した前立腺癌の放射線治療成績は比較的良好です．低リスク群では 70 Gy 程度の外部照射，小線源治療で治療可能ですが，中リスク群以上では 3D-CRT や IMRT により 70 Gy 以上の線量が必要です．治療法の選択は施設の状況，患者の希望などを加味して行うことが重要と考えます．

文献

1) 国立がんセンターがん対策情報センター http://www.ncc.go.jp/jp/cis/index.html
2) Zelefsky MJ, Yamada Y, Fuks Z et al. Long-term results of conformal radiotherapy for prostate cancer: impact of dose escalation on biochemical tumor control and distant metastases-free survival outcomes. *Int J Radiat Oncol Biol Phys* 2008; 71: 1028–1033
3) Hanks GE, Hanlon AL, Schultheiss TE et al. Dose escalation with 3D conformal treatment: five year outcomes, treatment optimization, and future directions. *Int J Radiat Oncol Biol Phys* 1998; 41: 501–510
4) Pollack A, Zagars GK, Starkschall G et al. Prostate cancer radiation dose response: results of M.D. Anderson phase III randomized trial. *Int J Radiat Oncol Biol Phys* 2002; 53: 1097–1105
5) Zelefsky MJ, Fuks Z, Hunt M et al. High-dose intensity modulated radiation therapy for prostate cancer: early toxicity and biochemical outcome in 772 patients. *Int J Radiat Oncol Biol Phys* 2002; 53: 1111–1116
6) Slater JD, Rossi CJ Jr, Yonemoto LT et al. Conformal proton therapy for early-stage prostate cancer. *Urology* 1999; 53: 978–984
7) Tsuji H, Yanagi T, Ishikawa H et al. Hypofractionated radiotherapy with carbon ion beams for prostate cancer. *Int J Radiat Oncol Biol Phys* 2005; 63: 1153–1160

臨床放射線 54：1705-1706，2009

はじめに

本田憲業*1　小川芳弘*2

FDG PET/CT複合機検査（以下PET/CT）は悪性腫瘍の診療に，革命をもたらしつつあると考えられる。米国でFDG PET/CTの適応拡大のために行われた，がん登録を用いた研究では全対象の約36%で治療方針の変更があったと報告されている[1]。がん患者三人に一人強がFDG PET/CTの利用によって治療方針が変わることになり，がん診療が大きな影響をうけることが明白である。がん対策基本法が制定され，がん診療の一層の向上が要望されるわが国では，FDG PET/CTの利用は必要不可欠と考えられるデータである。しかるに，わが国のPET/CT検査料は医療機関が赤字を被るほどの安価[2][3]に制限されており，結果，PET/CTの普及は十分ではなく，PET/CTを行わないで治療方針をたてるがん患者が相当数存在するのが現実である。したがって，がん診療においてFDG PET/CT利用の推進をはかることは核医学にたずさわるものにとって大きな課題である。

本特集は2009年春，第68回日本医学放射線学会にて開催されたシンポジウム5（2009年4月18日開催）の内容をまとめたものである。シンポジウムはがん診療へのFDG PET/CT利用の新しい展開を提示していただくことをねらいに企画したものである。話題をPET/CTに限ったのは，米国での適応拡大研究でも検査の87.3%はPET/CTで行われていること[1]，わが国の新規PET購入のほとんどはPET/CT複合機であって今後の主役はPET単独機でなくPET/CT複合機と目されること，さらには，放射線外照射治療への利用には解剖学的情報が同時に得られるPET/CTが必須と思われること，等を考慮したためである。

核医学を専攻されている二人の著者（鳥塚，立石両先生）にはFDG PET/CTがん病期診断の最新事情，および，呼吸運動がPET/CT画像に影響をあたえ放射線治療上も特別な配慮を要することを踏まえた，現時点での取り組みについて報告していただいた。放射線腫瘍学の立場からは，頭頸部と胸部のがん治療を実施している三人の著者（高井，高橋，青木先生）にお願いして，各領域でのPET/CT利用の現状と将来展望を示していただいている。シンポジウム，および，本特集での報告に示されるごとく，放射線外照射へのFDG PET/CTへの適応はまだ始まったばかりである。このシンポジウムを機会にこの方面の関心を高め多くの研究が展開されることを願っている。

PET/CT複合機で始まった融合画像は今後別種の融合画像へと一層の発展をみると予想される。すでに核医学ではSPECT/CT複合機が市販されわが国でも使用実績がある。核医学融合画像の威力を知った核医学医はPETあるいは，SPECT単独の画像に戻ることはできないとの実感を聞く機会が多い。また，PET/MRI複合機の開発を進めている画像診断機器メーカもある。このような画像融合の次に目指すべきは，医学領域の融合である。異なる領域が融合画像を「かすがい」に有機的に結合して医学・

*1 N. Honda　埼玉医科大学総合医療センター放射線科　*2 Y. Ogawa　東北大学放射線腫瘍学分野
〔索引用語：PET/CT〕

医療に改善や進歩をもたらすことが期待される。腫瘍放射線学と核医学はまさに，このような望ましい医学領域の融合と考えられる。

放射線治療の分野では，近年の治療機器，治療技術の進歩によって，高精度の放射線治療が可能になっている。この高精度照射技術を生かして放射線治療効果を高めるには，いかに病巣をはずさずに放射線を集中できるかが重要である。多くの施設では，それを実現させるためにCT，MRIを用いた三次元的治療計画を行い，肺癌の定位照射では手術に匹敵する成績も報告されている。CT，MRIでは腫瘍の局在，形態は把握しやすいが，リンパ節転移などは，大きさで判断せざるを得ないことも多く，照射野決定に悩むことも多い。そこで，近年脚光を浴びているのがPETである。PETは組織の代謝系をみることができ，腫瘍の局在，悪性度などを判断するのに有用であるとされている。しかし，PET画像では核医学画像の性格上辺縁がはっきりせず，そのままでは放射線治療計画に利用するのは難しい。そこに登場したのがPET/CTである。CTにPET画像をfusionさせた画像は治療計画装置に転送して計画することが可能である。

もちろん，PET/CTの空間分解能や位置精度，治療計画装置との接続等，超えなければならないハードルはあるが，それらがクリアできれば，PET/CTと，高精度照射技術の融合でもたらされる利益は相当なものであると考える。たとえば，無気肺を伴った肺癌では，通常のCT，MRIではどこまで腫瘍か，どこからが，無気肺かの判断は非常に難しいことが多く，実際の照射は無気肺領域をかなり多く含んだ大きな照射野になってしまう。それがPET/CTでは腫瘍部分と無気肺部分が区別できる可能性がある。頭頸部腫瘍では，頸部リンパ節転移の判断に有用とも言われている。PET/CTを有効に利用して，適切な標的を決めることが可能になるわけである。また，糖代謝をみるFDG以外にも，放射線が効きにくいとされる低酸素細胞を検出しうる薬剤の開発も進んでいる。昨今急速に利用が始まっている強度変調照射法（IMRT）を利用して，腫瘍のうちviable cellが多く存在する部位や，低酸素細胞が存在する領域に，より多くの線量を集中させることで，治療効果を高めることが期待できる。

PET/CTを治療計画に有効に用いるためには，PET/CTをよく理解することが必要である。最近最も多く利用されているのがFDG PET/CTであるが，FDGの集積の度合はSUV（standardized uptake value）で表現されることが多い。SUVはあくまで相対的な数値であり，その数値がいくつ以上なら悪性かというのは，難しい識論である。呼吸性移動に伴うSUVのばらつきも考慮する必要がある。それらをふまえて，標的を決める訳だが，実際の治療計画においては，計画者の判断がまちまちになり，計画者によって照射野サイズが違ってきてしまうということが出てくる可能性がある。治療医が期待するのは，PET/CTによっていかに病巣にしぼり，線量集中させるための照射野が設定できるかである。誰が計画を立てても同じ結果になるような指標が必要であろう。

PET/CTが放射線治療に与える影響は非常に大きいと考える。我々治療医はできればたくさんの症例に応用したいと考えている。今回のシンポジウムでは，PET/CTについての知識を再確認し，その有用性や，問題点等につき識論を深められたと思う。PET/CTが放射線治療計画にもたらしうる利益は計り知れないものがある。保険診療の制限，DPCの制限など地道にクリアしていかなければならない問題もあるが，今後のPET/CTと放射線治療計画の融合のさらなる発展を期待したい。

文　献

1) Hillner BE et al：Impact of positron emission tomography/computed tomography and positron emission tomography (PET) alone on expected management of patients with cancer：Initial results from the national oncologic PET registry. J Clin Oncology 26：2155-2161, 2008
2) 満武巨裕ほか：PET施設の医療経営：全国価格調査および3施設費用調査データに基づく分析．核医学 44：125-129, 2007
3) 満武巨裕ほか：PET施設の医療経営：デリバリーFDG利用施設における費用分析．核医学 45：119-123, 2008

Foreword：Harmony of PET/CT and radiotherapy planning

Norinari Honda[*1], *Yoshihiro Ogawa*[*2]
*1 *Department of Radiology*
Saitama Medical Center, Saitama Medical School
*2 *Department of Radiation Oncology*
Tohoku University Graduate School of Medicine

ELSEVIER

Int. J. Radiation Oncology Biol. Phys., Vol. 74, No. 2, pp. 349–354, 2009

0360-3016/09/$–see front matter

doi:10.1016/j.ijrobp.2008.08.072

CLINICAL INVESTIGATION **Lung**

EXTRAPULMONARY SOFT-TISSUE FIBROSIS RESULTING FROM HYPOFRACTIONATED STEREOTACTIC BODY RADIOTHERAPY FOR PULMONARY NODULAR LESIONS

TAKATSUGU KAWASE, M.D., PH.D.,* ATSUYA TAKEDA, M.D., PH.D.,†‡ ETSUO KUNIEDA, M.D., PH.D.,*‡ MASAKI KOKUBO, M.D., PH.D.,§ YOSHIFUMI KAMIKUBO, R.T.T.,¶ RYOUCHI ISHIBASHI, M.D.,¶ TOMOAKI NAGAOKA, PH.D.,‖ NAOYUKI SHIGEMATSU, M.D., PH.D.,* AND ATSUSHI KUBO, M.D., PH.D.*

*Department of Radiology, Keio University School of Medicine, Tokyo, Japan; †Department of Radiology, Ofuna Chuo Hospital, Kamakura, Japan; ‡Department of Radiology, Tokyo Metropolitan Hiroo Hospital, Tokyo, Japan; §Division of Radiation Oncology, Department of Image-Based Medicine, Institute of Biomedical Research and Innovation, Kobe, Japan; ¶Department of Radiology, Federation of National Public Service Personnel Mutual Aid Associations, Tachikawa Hospital, Tachikawa, Japan; and ‖National Institute of Information and Communications Technology, Koganei, Japan

Purpose: To clarify the incidence, symptoms, and timing of extrapulmonary fibrosis developing after hypofractionated stereotactic body radiotherapy.

Patients and Methods: We analyzed 379 consecutive patients who underwent stereotactic body radiotherapy for lung tumors at four institutions between February 2001 and March 2007. The median follow-up time was 29 months (range, 1–72). We investigated the subjective and objective characteristics of the extrapulmonary masses, redelineated the origin tissue of each on the treatment planning computed tomography scan, and generated dose–volume histograms.

Results: In 9 patients (2.4%), extrapulmonary masses were found 3–36 months (median, 14) after irradiation. Coexisting swelling occurred in 3 patients, chest pain in 2, thumb numbness in 1, and arm edema in 1 patient. Extrapulmonary masses occurred in 5 (5.4%) of 92 and 4 (1.4%) of 287 patients irradiated with a 62.5-Gy and 48.0-Gy isocenter dose, respectively. The mean and maximal dose to the origin tissue was 25.8–53.9 Gy (median, 43.7) and 47.5–62.5 Gy (median, 50.2), respectively. In 5 of 9 patients, the standardized uptake values on 18F-fluorodeoxyglucose-positron emission tomography was 1.8–2.8 (median, 2.2). Percutaneous needle biopsy was performed in 3 patients, and all the specimens showed benign fibrotic changes without malignant cells.

Conclusion: All patients should be carefully followed after stereotactic body radiotherapy. The findings of any new lesion should prompt an assessment for radiation-induced extrapulmonary fibrosis before an immediate diagnosis of recurrence is made. Careful beam-shape modification and dose prescription near the thoracic outlet are required to prevent forearm neuropathy and lymphedema. © 2009 Elsevier Inc.

Radiation toxicity, Fibrosis, Stereotactic body radiotherapy, Lung cancer.

INTRODUCTION

High-dose hypofractionated stereotactic body radiotherapy (SBRT) has recently been adopted into clinical use as radical RT for early-stage non–small-cell lung cancer (1–6). However, in addition to large antitumor effects, SBRT has also been found to produce various acute and subacute adverse reactions (2, 7–13). In addition to these events, we have observed that tumorous soft-tissue fibrosis can occur in the chest wall near the RT target volume. Although soft-tissue fibrosis after conventional RT is well-known (14–17), such pathologic effects have rarely been encountered in patients treated with SBRT and have not been the subject of any formal study.

In this study, we retrospectively analyzed consecutive cases of localized primary or metastatic lung cancer treated with SBRT at four different institutions to clarify the incidence, clinical symptoms, and timing of the appearance of soft-tissue masses after SBRT.

PATIENTS AND METHODS

We analyzed 379 consecutive patients (with 388 lesions) who underwent SBRT at four institutions for isolated T1-T2N0M0 primary

Reprint requests to: Etsuo Kunieda, M.D., Ph.D., Department of Radiology, Keio University School of Medicine, 35 Shinanomachi, Shinjuku-ku, Tokyo 160-8582 Japan. Tel: (+81) 3-3353-1211; ext. 62531; Fax: (+81) 3-3359-7425; E-mail: kunieda-mi@umin.ac.jp

Presented in part as a poster at the 49th Annual Meeting of the American Society for Therapeutic Radiology and Oncology (ASTRO), October 28–November 1, 2007, Los Angeles, CA.

Conflict of interest: none.

Received June 12, 2008, and in revised form Aug 13, 2008. Accepted for publication Aug 14, 2008.

or metastatic lung tumors ≤3 cm in maximal diameter between February 2001 and March 2007. The patient age range was 49–91 years (median, 74).

In brief, RT planning for SBRT was done as follows. Computed tomography (CT) scans were obtained with patient immobilization. Internal target volumes were determined directly by long-scan-time CT (18) or by "slow" CT (6–8 s/slice). The planning target volumes were delineated by adding 5- to 8-mm three-dimensional margins to the internal target volumes. Pinnacle^3 (Koninklijke Philips Electronics, Eindhoven, The Netherlands) or XiO (CMS, St. Louis, MO) was used as the RT planning system. The collapsed-cone algorithm of Pinnacle^3 or the multigrid superposition algorithm of XiO with a density heterogeneity correction was used. The following dose prescriptions were used: 50 Gy (at 80% isodose line) delivered in five fractions within 5–8 days with dynamic conformal multiple arcs (Institutions A and B) or 48 Gy (at isocenter) delivered in four fractions with six to eight three-dimensional static portals (Institutions C and D).

The median follow-up time was 29 months (range, 1–72). Whole-chest CT scans were obtained every 3 months for 2 years and every 4–6 months after 2 years. Additional scanning was done when clinically necessary. Subjective findings, as well as objective findings detected by palpation or clinical radioimaging, were used as the study endpoints. 18F-Fluorodeoxyglucose-positron emission tomography (FDG-PET) was performed in patients whose soft-tissue masses were suspected to be recurrent lesions. We reviewed all CT images of the patients who were suspected to have soft-tissue masses on the basis of the physical examination or CT findings. In such cases, we redelineated the origin tissues (*i.e.*, the origin of the soft-tissue mass) from the treatment planning CT data obtained with the RT planning systems to yield the dose–volume histograms (DVHs) in the patients with soft-tissue masses. Furthermore, biologically effective doses (BEDs) (19) with an α/β ratio of 3 Gy (20) were obtained to represent the radiation dose to the origin tissues. The Spearman correlation coefficient (two-sided) was used to examine the relationship between the mean BED and the volume of the origin tissues using the Statistical Package for Social Sciences, version 14.0 (SPSS, Chicago, IL).

RESULTS

Soft-tissue masses were found in the chest wall of 9 (2.4%) of the 379 patients. The lesions were detected on CT 3–36 months (median, 14) after RT. In 6 patients whose soft-tissue lesions were found subjectively, this occurred 3–21 months (median, 10.5) after RT. In 3 patients without subjective findings, the masses were found on follow-up CT scans 15–36 months (median, 24) after RT.

The patient characteristics and radiation doses prescribed for the lung tumors are given in Table 1. The clinical target volume was located in the upper lobes in 7 patients and in the lower lobes in 2. Soft-tissue masses were found in 5 (5.4%) of 92 patients whose target lesions were irradiated with 62.5 Gy in five fractions as an isocenter dose compared with 4 (1.4%) of 287 patients whose target lesions were irradiated with 48.0 Gy in four fractions as an isocenter dose.

The details of the radiation-induced soft-tissue masses and findings from the follow-up examinations are presented in Table 2. All the DVHs of the origin tissue are shown in Fig. 1. The origin tissue volumes were 1.4–16.4 cm^3 (median, 6.9). The mean doses to the origin tissue were 25.8–53.9 Gy (median, 43.7). The maximal doses to the origin tissues were 47.5–62.5 Gy (median, 50.2). The volume of the origin tissues vs. the mean BED is plotted in Fig. 2. A negative correlation between these two variables was observed.

The soft-tissue masses were detected by CT concurrently with, or subsequent to, the occurrence of symptoms in the 6 symptomatic patients. The symptoms consisted of a swollen chest wall in 3 patients, ipsilateral chest pain in 2, ipsilateral thumb numbness in 1, and ipsilateral arm edema in 1 patient.

The FDG-PET examinations were conducted 16–36 months (median, 24) after RT in 5 of 9 patients whose soft-tissue masses were suspected to be local recurrences. The studies were performed 0–20 months (median, 4) after the subjective or objective detection of the soft-tissue masses. The standardized uptake values of FDG-PET in the patients was 1.8–2.8 (median, 2.2). Subsequently, 3 of 5 patients who had undergone a PET study underwent percutaneous needle biopsy of the lesion 16–38 months (median, 19) after RT. All of the pathology findings showed only benign soft-tissue fibrotic changes and no malignant cells.

The follow-up period in 9 patients who had soft-tissue masses was 15–61 months (median, 35). At the end of the follow-up period, 7 patients were alive without locoregional recurrence or distant metastasis and 2 were alive with disease. In the 2 patients with disease, 1 had ipsilateral hilar metastatic adenopathy and 1 had local tumor recurrence. The CT findings in 2 representative cases of soft-tissue masses are shown in Figs. 3 and 4.

Table 1. Patient characteristics

Pt. No.	Age (y)	Gender	Primary/ Metastasis	Tumor location	Histopathologic finding	Isocenter dose (Gy/Fx)
1	60	Female	Primary	LUL	SCC	62.5/5
2	70	Male	Primary	RUL	Adenocarcinoma	62.5/5
3	82	Male	Primary	LUL	SCC	62.5/5
4	62	Female	Primary	RUL	Adenocarcinoma	64.5/5
5	76	Female	Primary	LUL	Adenocarcinoma	64.8/5
6	62	Male	Primary	LUL	Adenocarcinoma	48.0/4
7	86	Female	Primary	RLL	Adenocarcinoma	47.5/4
8	86	Male	Metastasis	LUL	SCC	48.0/4
9	79	Male	Primary	LLL	Adenocarcinoma	48.0/4

Abbreviations: Pt. No. = patient number; Fx = fraction; LUL = left upper lobe; SCC = squamous cell carcinoma; RUL = right upper lobe; RLL = right upper lobe; LLL = left lower lobe.

Table 2. Clinical, pathologic, irradiation, and postirradiation characteristics of patients with soft-tissue fibrotic masses

Pt. No	Estimated absorbed dose* (Gy)	Fibrosis volume (cm^3)	Symptom breakout (mo)/local symptom	Objective fibrosis breakout (mo)	FDG-PET (mo)/SUV	Biopsy timing (mo)/ histopathologic finding	Follow-up (mo)/prognosis
1	25.8 (70.2)/49.9 (216)	7.3	3/Swelling	8	16/2.2	19/fibrosis	44/NR
2	53.9 (248)/62.2 (320)	5.9	Asymptomatic	36	36/2.8	38/fibrosis	61/NR
3	50.6 (221)/61.0 (309)	2.1	21/Swelling	21	NA	NA	43/NR
4	47.0 (194)/62.5 (323)	6.9	2/Thumb numbness	3	NA	NA	30/WD
5	32.7 (104)/62.5 (323)	16.4	7, 13/chest pain, arm edema	14	27/2.3	NA	28/NR
6	39.9 (173)/50.2 (260)	12.7	12/swelling	13	16/1.8	16/fibrosis	43/NR
7	43.7 (203)/47.5 (236)	1.4	6/chest pain	6	NA	NA	15/NR
8	46.8 (229)/50.1 (259)	6.5	Asymptomatic	15	NA	NA	35/WD
9	43.6 (202)/47.9 (239)	7.1	Asymptomatic	24	24/2.1	NA	25/NR

Abbreviations: Pt. No. = patient number; FDG-PET = 18F-fluorodeoxyglucose-positron emission tomography; SUV = standard uptake value; NA = not available; NR = alive without recurrence; WD = alive with disease.

* Data presented as mean/maximal dose at fibrosis with calculated biologically effective dose (α/β ratio, 3 Gy) in parentheses.

DISCUSSION

Adverse events due to SBRT can be classified into two types according to the location in the lung where they arise. The first type arises in the pulmonary centrums near or next to the mediastinum, and the second type arises in the pulmonary periphery. The first type is associated with severe and lethal radiation injuries, including radiation esophagitis (2, 7, 9), radiation bronchitis (2, 8), and pulmonary artery hemorrhage (2). In addition, Timmerman *et al.* (12) have strongly emphasized that great care must be taken in performing SBRT when the targets are located near the pulmonary hilum because of the high incidence of Grade 5 secondary bacterial pneumonia in such patients. Adverse events that arise in the pulmonary periphery (type 2 events) include rib fractures (10) and chest pain (11). The adverse events found in our study, namely soft-tissue masses causing chest pain, forearm neuropathy, and lymphedema, also qualify as the second type of event. Although adverse events resulting from SBRT might not directly affect the prognosis, the adverse events we found can cause the clinical issues described in our study.

A soft-tissue mass in the absence of marked chest pain was observed in several of the patients in our series, with analgesics not needed for patients with only slight chest pain. Chest pain after SBRT can also occur in patients who do not have any soft-tissue mass (3, 7, 11). Therefore, chest wall pain is not always indicative of a soft-tissue mass. A fibrotic mass

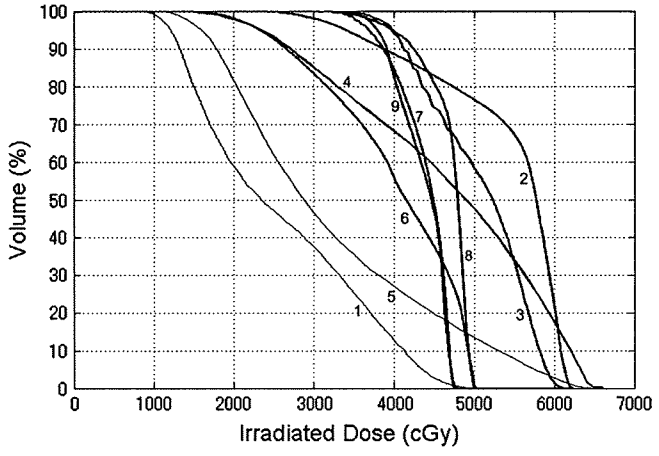

Fig. 1. Dose–volume histogram (DVH) of origin tissues (*i.e.*, origin of soft-tissue mass). With regard to follow-up computed tomography images showing soft-tissue masses, contour of volume redelineated on treatment planning computed tomography images to calculate DVH. Two groups of curves noted. Seven curves (heavy lines) represent therapeutic, high-dose, uniform irradiation to volumes. Other two curves (thin lines) indicate gradually increasing irradiation from low to high dose. Consecutive numbers near DVH curves correspond to patient numbers in Tables 1 and 2.

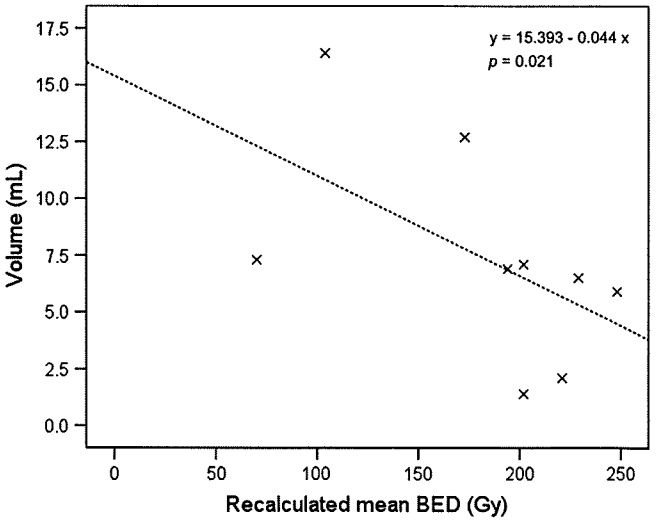

Fig. 2. Relationship of recalculated mean biologically effective dose (BED) to volume of origin tissue. In calculating BEDs, α/β ratio of 3 Gy was assumed for late reaction of normal tissue of chest wall. Negative correlation between these two variables observed (Spearman $r = -0.745$, $n = 9$, $p = .021$).

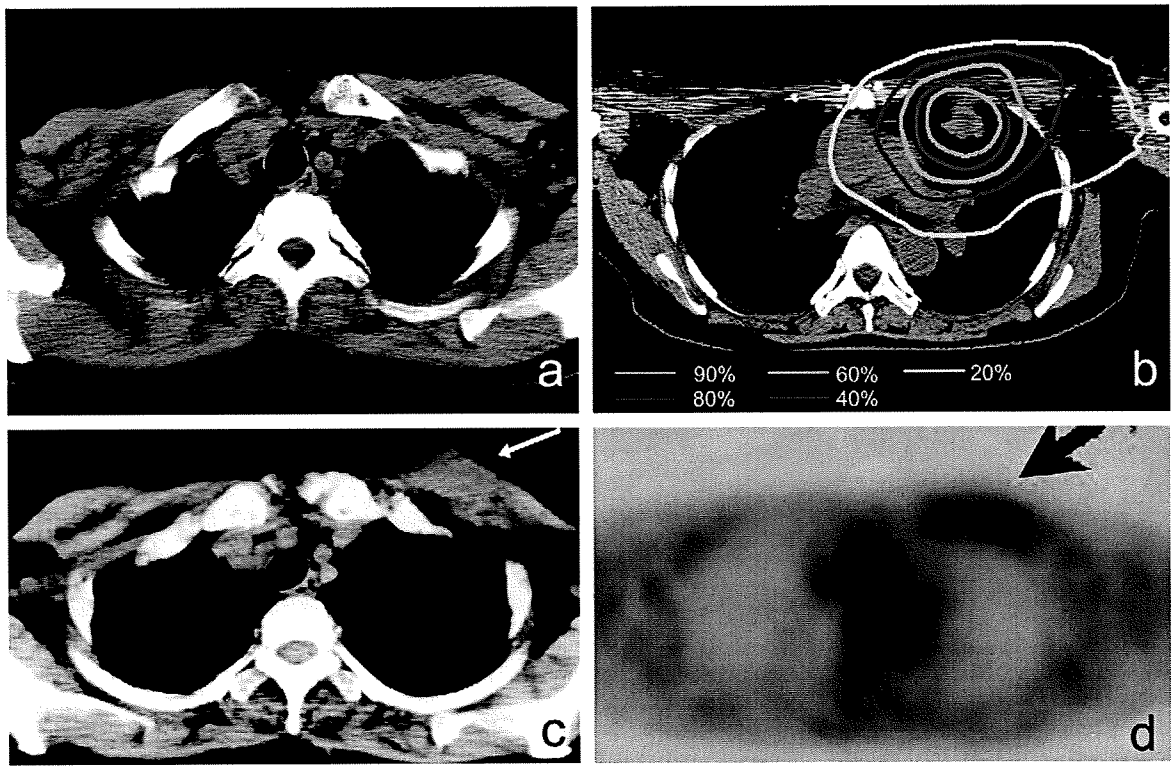

Fig. 3. Case of primary lung, Stage cT1N0M0, squamous cell carcinoma in left upper lobe (Patient 1 in Tables 1 and 2). Axial computed tomography image before (a) irradiation and (b) isodose distributions. The second curve from inside indicates 80% isodose and corresponds with planning target volume. Patient was aware of subcutaneous swelling on left side of front chest about 3 months after irradiation. (c) Follow-up computed tomography study showed soft-tissue mass around ribs and in left greater pectoral muscle that continued to enlarge. (d) 18F-Fluorodeoxyglucose-positron emission tomography study at 16 months after irradiation showed localized uptake (standardized uptake value, 2.2) corresponding to the lesion. Percutaneous needle biopsy specimen revealed fibrosis and not malignant lesion. No clear recurrence was detected after that.

that arises in a noncritical region is likely to have a minimal affect on a patient's quality of life. However, a fibrotic lesion around the brachial plexus might cause forearm neuropathy and lymphedema (21–24), which, although not life-threatening, will affect a patient's quality of life. To prevent these sequelae, beam-shape modification and dose prescription must be done in such a way during the planning of SBRT for a tumor in the lung periphery that the beam does not pass through the areas near the subclavian and axillary regions.

The pathoetiology of brachial plexus neuropathy has not been clearly elucidated in patients who undergo SBRT. In breast cancer patients treated with conventional RT, both perineural fibrotic entrapment and direct nerve injury have been documented as causes of brachial plexus neuropathy (22). The pathology findings after intraoperative RT with a single high-fraction dose might also shed light on the etiology of brachial plexus neuropathy in patients who underwent SBRT. In this regard, Kinsella *et al.* (25) claimed that both nerve entrapment by perineural fibrosis and direct nerve injury could be the causes of neurologic impairment after RT with a single high-fraction dose observed in a canine model. In another canine model, Vujaskovic *et al.* (26) observed that axon and myelin loss, increased nerve connective tissue, and loss of small vessels occurred after intraoperative RT. It is, therefore, possible that brachial plexus neuropathy induced by SBRT might have a pathoetiology similar to that seen by these other researchers. Additional research is necessary to clarify this issue.

Severe lymphedema of the ipsilateral arm was also observed in our study population. It is well-known that forearm lymphedema frequently occurs after RT of the axilla in breast cancer patients (27). Patients treated with conventional RT and SBRT are at appreciable risk of this adverse event. Thus, lymphedema in a location remote from the site of RT is not an uncommon sequela. Physical and manual massage (28) and microsurgical lymphatic venous anastomosis (29, 30) have been attempted as treatments for such lymphedema; however, none of these are definitive treatments.

Among the DVHs of the origin tissue for the 9 patients in our study with soft-tissue masses after SBRT, we noted seven curves representing high-dose uniform RT to the volumes and two other curves representing gradually increasing RT from a low dose to high dose. The former seven curves are believed to represent typical dose distributions for the adverse reactions focused on in the present study. In the case of the latter two curves, the soft-tissue fibrotic masses were located in muscle. In this setting, we might have included in the origin tissue not only the soft-tissue mass but also

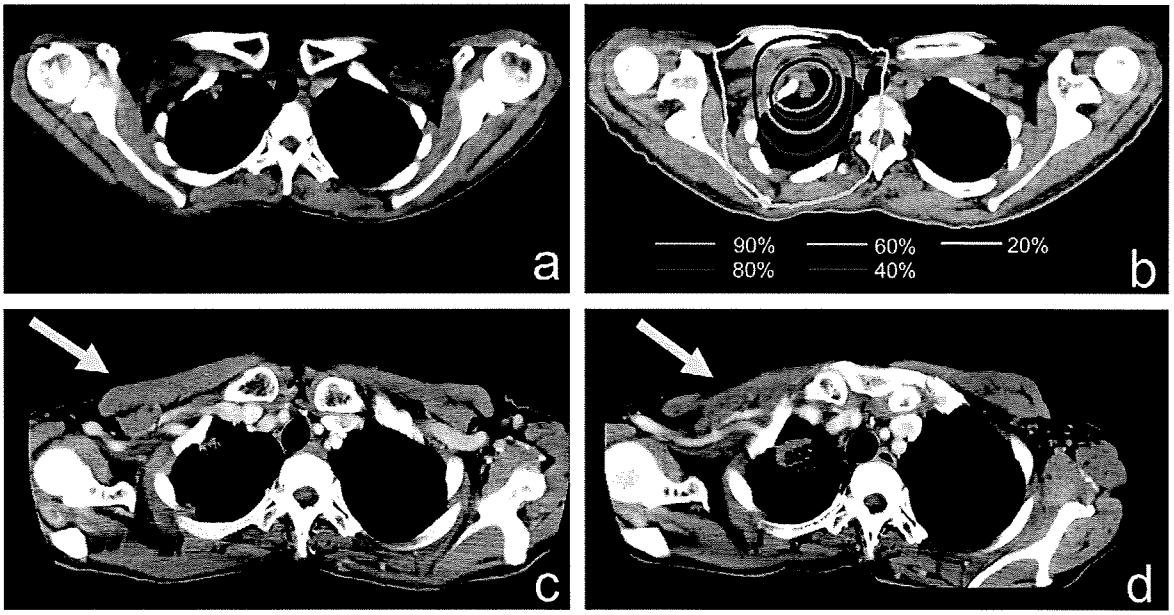

Fig. 4. Primary lung cancer (cT1N0M0, adenocarcinoma) in right upper lobe (Patient 4 in Tables 1 and 2). Axial computed tomography image before (a) irradiation and (b) isodose distributions. The second curve from inside indicates 80% isodose and corresponds with planning target volume. Patient complained of numbness of ipsilateral fingers 2 months after irradiation. Computed tomography images showed soft-tissue density in right axilla. (c,d) Subsequently, density enlarged and seen as soft-tissue mass on computed tomography (arrows). Patient had interdigital and thenar eminence muscle atrophy of ipsilateral hand 18 months after irradiation. These symptoms were diagnosed as neuropathy of brachial plexus resulting from soft-tissue mass. Soft-tissue mass grew until 17 months after irradiation, after which it stopped. Primary lesion also remained unchanged and was judged as well controlled. However, computed tomography 29 months after irradiation revealed ipsilateral hilar metastatic adenopathy.

muscular swelling near the target due to RT. Muscular swelling after RT has been reported to be a radiation injury (31, 32). Therefore, the volumes of the origin tissue in these 2 patients might have been overestimated, and this overestimation might have been the source of the leftward shift of the DVHs. In addition, a negative correlation was found between the volume of the origin tissue and the recalculated mean BED in all 9 patients. This suggests a volume effect resulting from this adverse event.

The formation of a soft-tissue mass in an extrapulmonary, as well as an intrapulmonary, location resulting from SBRT can be confused with recurrence or metastasis. One observation that can help distinguish between a benign and a malignant process is that intrapulmonary radiation fibrosis can occur $\geq$1 year after the completion of SBRT for lung cancer. In contrast, recurrence can occur sooner than this. However, even when CT is performed as an aid to the diagnosis of the lesion, it is often difficult to distinguish a soft-tissue mass from tumor recurrence, and CT findings can even be misinterpreted (33). FDG-PET also might not be helpful in this regard, because the standardized uptake value cutoff level for a recurrent lesion after RT for lung cancer has not been established (34–36). Therefore, percutaneous needle biopsy was necessary in some cases in our study to establish the true nature of the lesion.

Recurrent lung tumors in the thorax often take the form of local tumor regrowth, pleural dissemination, or thoracic bone metastasis. It is rare for recurrences to arise in the soft tissue of the chest wall apart from but near the primary tumor site. In our study, we found soft-tissue masses in the chest wall in 9 (2.4%) of 379 patients after RT, and all the lesions were diagnosed as benign fibroses. Thus, when an unexpected extrapulmonary soft-tissue mass is found after SBRT, it should not immediately be judged a recurrence. Soft-tissue fibrosis should also be considered.

CONCLUSIONS

A soft-tissue mass was found in 2.4% of patients in our study population who had undergone SBRT for pulmonary tumors in the chest wall near the planning target volume. In all these patients, the masses proved to be radiation fibroses and not recurrences. Forearm neuropathy and lymphedema were common symptoms and resulted because the soft-tissue masses arose near the brachial plexus. Careful beam-shape modification and dose prescription are required for target lesions located near the thoracic outlet to prevent these complications. We recommend careful follow-up of patients after SBRT that includes surveillance for radiation-induced extrapulmonary soft-tissue masses. If such masses are found, they should not immediately be judged as recurrences, however.

REFERENCES

1. Uematsu M, Shioda A, Tahara K, *et al.* Focal, high dose, and fractionated modified stereotactic radiation therapy for lung carcinoma patients: A preliminary experience. *Cancer* 1998;82: 1062–1070.
2. Wulf J, Hadinger U, Oppitz U, *et al.* Stereotactic radiotherapy of targets in the lung and liver. *Strahlenther Onkol* 2001;177: 645–655.
3. Uematsu M, Shioda A, Suda A, *et al.* Computed tomography-guided frameless stereotactic radiotherapy for stage I non–small-cell lung cancer: A 5-year experience. *Int J Radiat Oncol Biol Phys* 2001;51:666–670.
4. Timmerman R, Papiez L, McGarry R, *et al.* Extracranial stereotactic radioablation: Results of a phase I study in medically inoperable stage I non-small cell lung cancer. *Chest* 2003;124: 1946–1955.
5. Onishi H, Araki T, Shirato H, *et al.* Stereotactic hypofractionated high-dose irradiation for stage I nonsmall cell lung carcinoma: Clinical outcomes in 245 subjects in a Japanese multi-institutional study. *Cancer* 2004;101:1623–1631.
6. Takeda A, Sanuki N, Kunieda E, *et al.* Stereotactic body radiotherapy for primary lung cancer at a dose of 50 Gy Total in five fractions to the periphery of the planning target volume calculated using a superposition algorithm. *Int J Radiat Oncol Biol Phys* 2009;73:442–448.
7. Onimaru R, Shirato H, Shimizu S, *et al.* Tolerance of organs at risk in small-volume, hypofractionated, image-guided radiotherapy for primary and metastatic lung cancers. *Int J Radiat Oncol Biol Phys* 2003;56:126–135.
8. Uno T, Aruga T, Isobe K, *et al.* Radiation bronchitis in lung cancer patient treated with stereotactic radiation therapy. *Radiat Med* 2003;21:228–231.
9. Bradley J, Graham MV, Winter K, *et al.* Toxicity and outcome results of RTOG 9311: A phase I-II dose-escalation study using three-dimensional conformal radiotherapy in patients with inoperable non–small-cell lung carcinoma. *Int J Radiat Oncol Biol Phys* 2005;61:318–328.
10. Zimmermann FB, Geinitz H, Schill S, *et al.* Stereotactic hypofractionated radiation therapy for stage I non-small cell lung cancer. *Lung Cancer* 2005;48:107–114.
11. Nyman J, Johansson KA, Hulten U. Stereotactic hypofractionated radiotherapy for stage I non-small cell lung cancer—Mature results for medically inoperable patients. *Lung Cancer* 2006;51:97–103.
12. Timmerman R, McGarry R, Yiannoutsos C, *et al.* Excessive toxicity when treating central tumors in a phase II study of stereotactic body radiation therapy for medically inoperable early-stage lung cancer. *J Clin Oncol* 2006;24:4833–4839.
13. Takeda A, Enomoto T, Sanuki N, *et al.* Acute exacerbation of subclinical idiopathic pulmonary fibrosis triggered by hypofractionated stereotactic body radiotherapy in a patient with primary lung cancer and slightly focal honeycombing. *Radiat Med* 2009;26:504–507.
14. Gong QY, Zheng GL, Zhu HY. MRI differentiation of recurrent nasopharyngeal carcinoma from postradiation fibrosis. *Comput Med Imaging Graph* 1991;15:423–429.
15. Becker M, Schroth G, Zbaren P, *et al.* Long-term changes induced by high-dose irradiation of the head and neck region: Imaging findings. *Radiographics* 1997;17:5–26.
16. O'Sullivan B, Levin W. Late radiation-related fibrosis: pathogenesis, manifestations, and current management. *Semin Radiat Oncol* 2003;13:274–289.
17. Davis AM, O'Sullivan B, Turcotte R, *et al.* Late radiation morbidity following randomization to preoperative versus postoperative radiotherapy in extremity soft tissue sarcoma. *Radiother Oncol* 2005;75:48–53.
18. Takeda A, Kunieda E, Shigematsu N, *et al.* Small lung tumors: Long-scan-time CT for planning of hypofractionated stereotactic radiation therapy—Initial findings. *Radiology* 2005;237: 295–300.
19. Fowler JF, Tome WA, Fenwick JD, *et al.* A challenge to traditional radiation oncology. *Int J Radiat Oncol Biol Phys* 2004; 60:1241–1256.
20. Johansson S, Svensson H, Denekamp J. Dose response and latency for radiation-induced fibrosis, edema, and neuropathy in breast cancer patients. *Int J Radiat Oncol Biol Phys* 2002;52: 1207–1219.
21. Olsen NK, Pfeiffer P, Mondrup K, *et al.* Radiation-induced brachial plexus neuropathy in breast cancer patients. *Acta Oncol* 1990;29:885–890.
22. Schierle C, Winograd JM. Radiation-induced brachial plexopathy: Review—Complication without a cure. *J Reconstr Microsurg* 2004;20:149–152.
23. Jaeckle KA. Neurological manifestations of neoplastic and radiation-induced plexopathies. *Semin Neurol* 2004;24:385–393.
24. Johansson S. Radiation induced brachial plexopathies. *Acta Oncol* 2006;45:253–257.
25. Kinsella TJ, DeLuca AM, Barnes M, *et al.* Threshold dose for peripheral neuropathy following intraoperative radiotherapy (IORT) in a large animal model. *Int J Radiat Oncol Biol Phys* 1991;20:697–701.
26. Vujaskovic Z, Powers BE, Paardekoper G, *et al.* Effects of intraoperative irradiation (IORT) and intraoperative hyperthermia (IOHT) on canine sciatic nerve: Histopathological and morphometric studies. *Int J Radiat Oncol Biol Phys* 1999;43: 1103–1109.
27. Meek AG. Breast radiotherapy and lymphedema. *Cancer* 1998; 83:2788–2797.
28. Brennan MJ, Miller LT. Overview of treatment options and review of the current role and use of compression garments, intermittent pumps, and exercise in the management of lymphedema. *Cancer* 1998;83:2821–2827.
29. Filippetti M, Santoro E, Graziano F, *et al.* Modern therapeutic approaches to postmastectomy brachial lymphedema. *Microsurgery* 1994;15:604–610.
30. Campisi C, Boccardo F. Frontiers in lymphatic microsurgery. *Microsurgery* 1998;18:462–471.
31. Gillette EL, Mahler PA, Powers BE, *et al.* Late radiation injury to muscle and peripheral nerves. *Int J Radiat Oncol Biol Phys* 1995;31:1309–1318.
32. Blomlie V, Rofstad EK, Tvera K, *et al.* Noncritical soft tissues of the female pelvis: Serial MR imaging before, during, and after radiation therapy. *Radiology* 1996;199:461–468.
33. Takeda A, Kunieda E, Takeda T, *et al.* Possible misinterpretation of demarcated solid patterns of radiation fibrosis on CT scans as tumor recurrence in patients receiving hypofractionated stereotactic radiotherapy for lung cancer. *Int J Radiat Oncol Biol Phys* 2008;70:1057–1065.
34. Patz EF Jr., Lowe VJ, Hoffman JM, *et al.* Persistent or recurrent bronchogenic carcinoma: Detection with PET and 2-[F-18]-2-deoxy-D-glucose. *Radiology* 1994;191:379–382.
35. Inoue T, Kim EE, Komaki R, *et al.* Detecting recurrent or residual lung cancer with FDG-PET. *J Nucl Med* 1995;36: 788–793.
36. Hoopes DJ, Tann M, Fletcher JW, *et al.* FDG-PET and stereotactic body radiotherapy (SBRT) for stage I non–small-cell lung cancer. *Lung Cancer* 2007;56:229–234.

Radiotherapy and Oncology 93 (2009) 45–49

Contents lists available at ScienceDirect

Radiotherapy and Oncology

journal homepage: www.thegreenjournal.com

Organ motion

Initial validations for pursuing irradiation using a gimbals tracking system

Kenji Takayama [a,b,c], Takashi Mizowaki [a,*], Masaki Kokubo [b], Noriyuki Kawada [c], Hiroshi Nakayama [c], Yuichiro Narita [a], Kazuo Nagano [b], Yuichiro Kamino [c], Masahiro Hiraoka [a]

[a] Department of Radiation Oncology and Image Applied Therapy, Kyoto University, Kyoto, Japan
[b] Institute of Biomedical Research and Innovation, Kobe, Japan
[c] Mitsubishi Heavy Industries Ltd., Tokyo, Japan

ARTICLE INFO

Article history:
Received 29 October 2008
Received in revised form 8 July 2009
Accepted 16 July 2009
Available online 21 August 2009

Keywords:
Pursuing irradiation
Gimbals tracking
Organ motion
Movable phantom
Image-guided radiotherapy (IGRT)

ABSTRACT

Our newly designed image-guided radiotherapy (IGRT) system enables the dynamic tracking irradiation with a gimbaled X-ray head and a dual on-board kilovolt imaging subsystem for real-time target localization. Examinations using a computer-controlled three-dimensionally movable phantom demonstrated that our gimbals tracking system significantly reduced motion blurring effects in the dose distribution compared to the non-tracking state.

Organ motion is an important issue during external-beam irradiation of extra-cranial lesions, particularly in the intra-thoracic and upper-abdominal regions, in which a tumor may move 1–2 cm as a result of respiration [1,2]. This motion results in blurred dose distributions and an enlarged beam penumbra at the radiation field edge [3,4]. Therefore, sufficiently large safety margins are required to compensate for motion effects when using conventional techniques. Several approaches have been used to minimize motion effects, including respiratory inhibition [5], breath-hold [6,7], respiratory gating [8–10], and tracking.

Real-time tracking irradiation is classified into two subcategories, according to the delivery scheme [2]. The first is intercepting irradiation, in which a therapeutic beam is gated to irradiate a tumor at a planned position by intercepting the tumor trajectory. This is in contrast to pursuing irradiation or dynamic tracking, which involves irradiating the target continuously as it moves through a three-dimensional (3D) space. Pursuing irradiation provides higher delivery efficiency and greater comfort than gating and intercepting irradiation, in which the relative low duty cycle (typically 30–50%) prolongs treatment time. In a robot-mounted linear accelerator (LINAC) system [11], pursuing irradiation is achieved through the use of a robotic arm, whereas dynamic multi-leaf collimator (DMLC)-based tracking utilizes a moving aperture [12]. Alternatively, a robotic couch moving in real time in response to organ motion has been considered [13], although this approach may be problematic in terms of patient discomfort and potential danger.

The image-guided radiation therapy (IGRT) system described here, which was designed for precise initial setup, high throughput, and pursuing irradiation of moving targets, was developed by Mitsubishi Heavy Industries in collaboration with Kyoto University and the Institute of Biomedical Innovation and Research. The system involves a novel gimbaled X-ray head that directs a multi-leaf collimator (MLC)-shaped beam to a designated point in real time. This paper describes a novel method for pursuing irradiation, termed "gimbals tracking", and provides data demonstrating its efficacy in reducing motion-induced marginal blurring.

Materials and methods

IGRT and the gimbals mechanism

The concept and configuration of this IGRT system using a gimbaled X-ray head were previously introduced by Kamino et al. [14]. Briefly, a compact, lightweight, C-band 6-megavolt (MV) LINAC was mounted on a gimbaled X-ray head with a MLC, and the entire moving unit was installed on a ring-shaped gantry within a crescent-shaped cover. The X-ray head can rotate along the two orthogonal gimbals (pan and tilt rotations) up to ±2.4°, which swings the MV beam up to ±4.2 cm in each direction from the

* Corresponding author. Address: Department of Radiation Oncology and Image Applied Therapy, Graduate School of Medicine, Kyoto University, 54 Kawahara-cho, Shogoin Sakyo-ku, Kyoto 606-8507, Japan.
E-mail address: mizo@kuhp.kyoto-u.ac.jp (T. Mizowaki).

0167-8140/$ - see front matter © 2009 Elsevier Ireland Ltd. All rights reserved.
doi:10.1016/j.radonc.2009.07.011

isocenter on the isocenter plane perpendicular to the beam. In the gimbals tracking mode, this mechanism enables the MV beam to track a target in real time. Two imaging units, each consisting of a kilovolt (kV) X-ray tube and a flat panel detector (FPD), were mounted on the gantry and provided real-time orthogonal serial radiographs. A gantry-mounted electronic portal imaging device (EPID) provided the information of the MV beam shape and position.

In this study, a prototype IGRT system was used. One of the differences from the commercial system was the MLC; the prototype used in this study had 40 pairs of 4-mm-thick leaves, which made a 16 × 16-cm field at the isocenter, whereas the commercial version had 30 pairs of 5-mm-thick leaves, which provide a 15 × 15-cm field.

Movable phantom system

A three-dimensionally movable phantom was developed to evaluate pursuing irradiation; the mechanical characteristics and accuracy of this system have been described previously [15]. The phantom system consisted of a drive unit, a computer control unit, and a spherical phantom (diameter, 19 cm). Radiographic film was inserted between the hemispheres of the phantom, and a copper plate was attached to the inside of the upper hemisphere to minimize film exposure. A pin-hole with a diameter of 2 mm at the center of the plate was used as a fiducial marker. The drive unit consisted of three linear stages designed to move the phantom according to the three-dimensional (3D) trajectory and velocity specified by the control unit.

Film irradiation

Irradiation tests using a prototype of our IGRT system were performed to evaluate the efficacy of gimbals tracking in reducing dose blurring. A 6-MV beam was used to irradiate an 8 × 8-mm field of film in the phantom under the following conditions:

(a) *Stationary state:* stationary phantom with a stationary X-ray head;
(b) *Non-pursuing state:* phantom in motion with a stationary X-ray head;
(c) *Pursuing irradiation:* phantom in motion with gimbals tracking enabled.

The phantom moved in the horizontal plane, parallel to the film and perpendicular to the MV beam. The following motion patterns were tested:

(1) linear reciprocal motion of a triangular wave (stroke, 20 mm; velocity, 10 mm/s);
(2) circular motion on the horizontal plane (radius, 10 mm; tangential velocity, 5 mm/s);
(3) linear reciprocal motion of a respiration-like wave (stroke, 20 mm).

During pursuing irradiation, the frame rate for real-time imaging was 7.5 frames/s, and an original predictive protocol based on a linear autoregressive model was applied to compensate for the mechanical and image processing lag of the tracking system. The Levinson–Durbin recursion algorithm was used to determine the coefficients of the model at a high speed [16]. This protocol allows prediction of the target position based on the past time series data and provides the gimbal control unit with positional information within milliseconds after obtaining the current position.

The irradiated film was developed, and its optical density was evaluated using a film analyzer. To mimic the clinical setting, motion effects in a 48 × 48-mm field were also examined, using a respiration-like wave, which was created from measured data for human abdominal wall motion.

Results

In every motion pattern, pursuing radiation using the method described here significantly reduced motion effects (*i.e.*, blurring). Fig. 1 shows the two-dimensional (2D) dose distributions and line dose profiles for an 8 × 8-mm field moving in a triangular wave or a circular motion. During linear reciprocal motion (Fig. 1 [1]), the 2D dose distribution for the phantom showed significant marginal blurring, reflecting the motion probability density function (PDF). Pursuing irradiation dramatically reduced blurring and produced a dose profile slope similar to that of the stationary state (<~1 mm). During circular motion (Fig. 1 [2]), a faint circular dose distribution was obtained; by contrast, pursuing irradiation produced a square dose distribution, similar to that of the stationary state, with only a slight marginal blurring in all directions.

Fig. 2 demonstrates the efficacy of pursuing irradiation while irradiating a 48 × 48-mm field in respiration-like motion. The stationary X-ray head produced significant blurring while the phantom was in motion. The high-dose area, defined as the distance between 95% dose points in the left and right slopes, decreased to approximately 70% (26.4/38.1) of the stationary state. The slope of the low-dose area, defined as the distance between 20% and 80% dose points, declined to approximately 5-fold that of the stationary state. During pursuing irradiation, blurring was so slight that the high-dose area was equivalent to the stationary state and the slope was only 1.5-fold that of the stationary state.

Discussion

The data presented here demonstrate the utility of gimbals tracking as a new method for pursuing irradiation. Gimbals tracking has three primary advantages. First, one-degree-ordered small-angle rotations of the gimbals provide quick and accurate beam adaptation to designated positions of a mobile target. Second, the mechanism is relatively simple and thus minimizes mechanical load. Finally, our system is safer than systems involving a robotic arm because the moving unit is covered.

However, we acknowledge that the beam path in the gimbals tracking system varies from the planned beam to some extent. This is one of the differences from the robot-mounted LINAC system, in which the beam path changes in parallel to the original path during beam tracking. Variation in the beam path is greatest when a target on the isocenter moves on a plane perpendicular to the beam. When the gimbaled head swings its maximum rotation by as much as 2.4° along both the pan and tilt axes of the gimbals, the target can be located 5.9 cm from the isocenter on the plane, and the distance between the target and radiation source is 100.2 cm. This discrepancy in distance compared to 100 cm means an approximate 1% dose change when calculated based on the percent depth dose (PDD) of the beam. Therefore, the effect of the beam path variation due to limited rotation of the gimbals appears to be reasonably small in terms of the dose. However, it would be better to simulate the impact of the described effects and to confirm whether possible dose differences are within clinically acceptable limits using a treatment planning system. Therefore, we plan to develop a treatment planning program for our system that will allow us to simulate and evaluate the dose distribution of tracking irradiation with a gimbal-mounted head.

In stereotactic body radiotherapy, gimbals tracking provides higher delivery efficiency than either gating or robotic tracking, and in comparison with robotic tracking it produces a more homo-

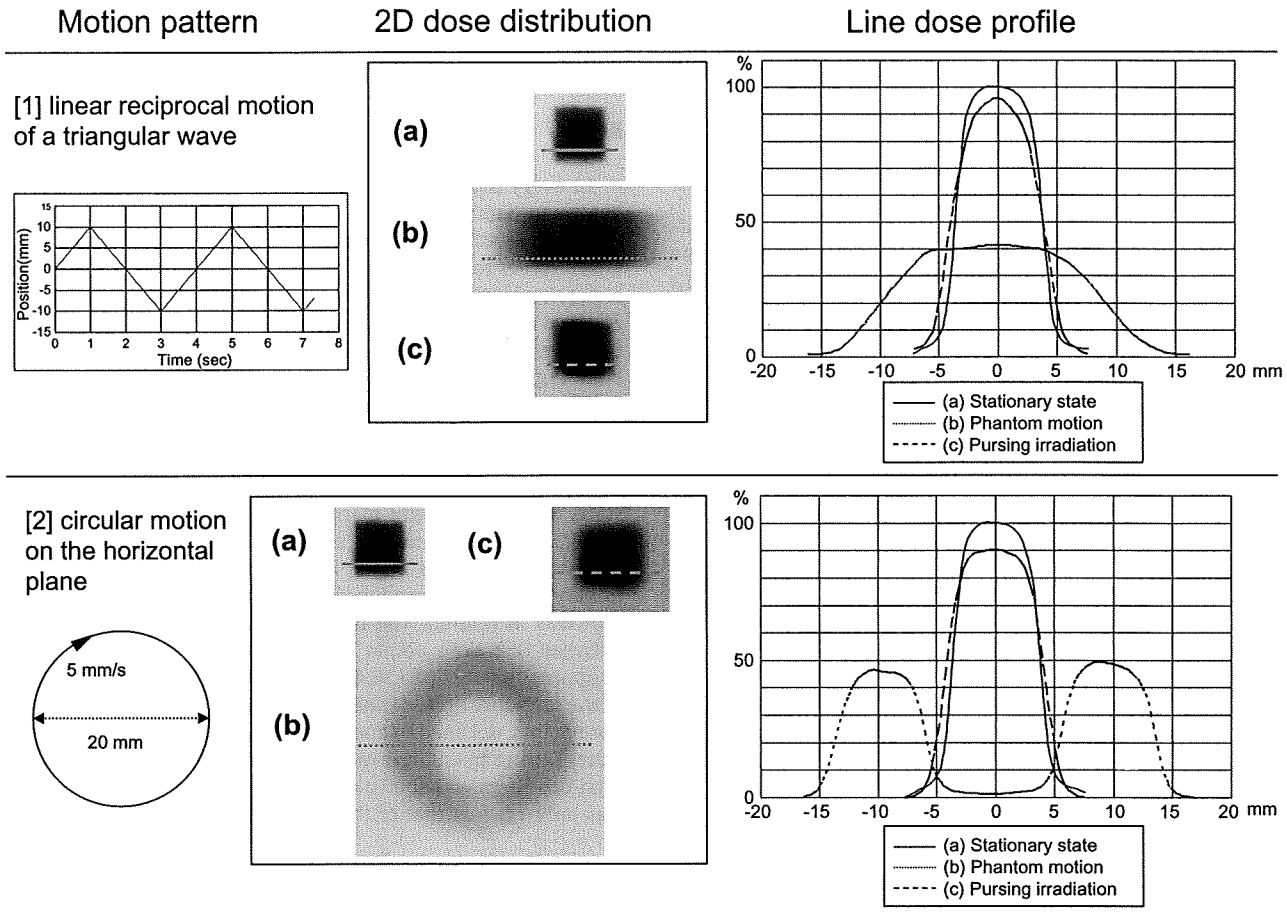

Fig. 1. Film irradiation experiments using an 8 × 8-mm field. Two-dimensional dose distributions and line dose profiles are shown for each motion pattern. After background compensation, the profiles were normalized for integral dose.

geneous in-field dose distribution, without cold spots. This is because, as in DMLC tracking, gimbals tracking uses ten or fewer flattened beams that are MLC-shaped to include the whole target in the beam's eye view. By contrast, robotic tracking is more time-consuming because several tens to 100 narrow conical beams are used, creating greater inhomogeneity in the dose distribution profiles compared with those of conventional MLC. Moreover, tracking error may occur independently in each beam, resulting in unpredictable hot and cold spots in the target.

Strictly speaking, the movement of a target in the human body involves both positional change and deformation. However, the deformation is relatively small for a small solitary tumor without lymph node metastasis, which is the most appropriate candidate for pursuing irradiation in general, rather than a large tumor, which may have a complex shape, subclinical extension, and lymph node metastasis. However, if deformation could be detected by an imaging system, such as a four-dimensional (4D) computed tomography (CT) scanner, a 4D treatment planning system considering these movements would help to cope with this issue. We have been developing an original 4D planning system at Kyoto University. If these technologies were available, gimbals tracking could be achieved by adjusting the irradiation fields to cover the entire target, including deformation. This is an advantage over a robot-mounted LINAC system, which would not easily compensate for deformation.

In terms of real-time imaging, our system uses a gantry-mounted stereo kV X-ray imaging system to detect real-time 3D positional information for a mobile target. This technique is capable of directly tracking tumors based on the density difference between the tumor and normal lung tissue, provided that the tumor is well defined with a high-contrast edge. Several variations of our tracking system would be possible in a clinical setting, such as direct tracking, external surrogates, and internal surrogates (fiducial markers, diaphragms, *etc.*). Further research is required to develop prediction techniques and correlation models for the surrogate signal versus internal tumor motion. The EPID allows visualization of the radiation field aperture and the tumor/internal surrogate, and thus may play an important role in verifying MV beam allocation.

Regarding the validation data presented in this study, our results showed that a 48 × 48-mm field produced a 38-mm high-dose area exposed to more than 95% of the dose in the stationary state (See Fig. 2). However, motion blurring in the non-pursuing state decreased the width of the high-dose area to 26.4 mm, which theoretically means that the field size in the target motion direction should have been enlarged to about 60 mm to create a similarly sized high-dose area. With pursuing irradiation, even if the slight marginal blurring is considered, a 50-mm field was large enough to create the same high-dose area. The slight blurring demonstrated in this study arose for several reasons, such as delays in image processing and communication, prediction error, and a mechanical response time lag. In fact, the response delay of the gimbals during the actual test was a maximum of 0.4–0.6 mm to sinusoidal motion, as mentioned in Kamino et al. [14]. Further investigation of these factors would improve the tracking accuracy of our system. Another solution to improve prediction accuracy may be to increase the sampling rate or imaging frame rate.

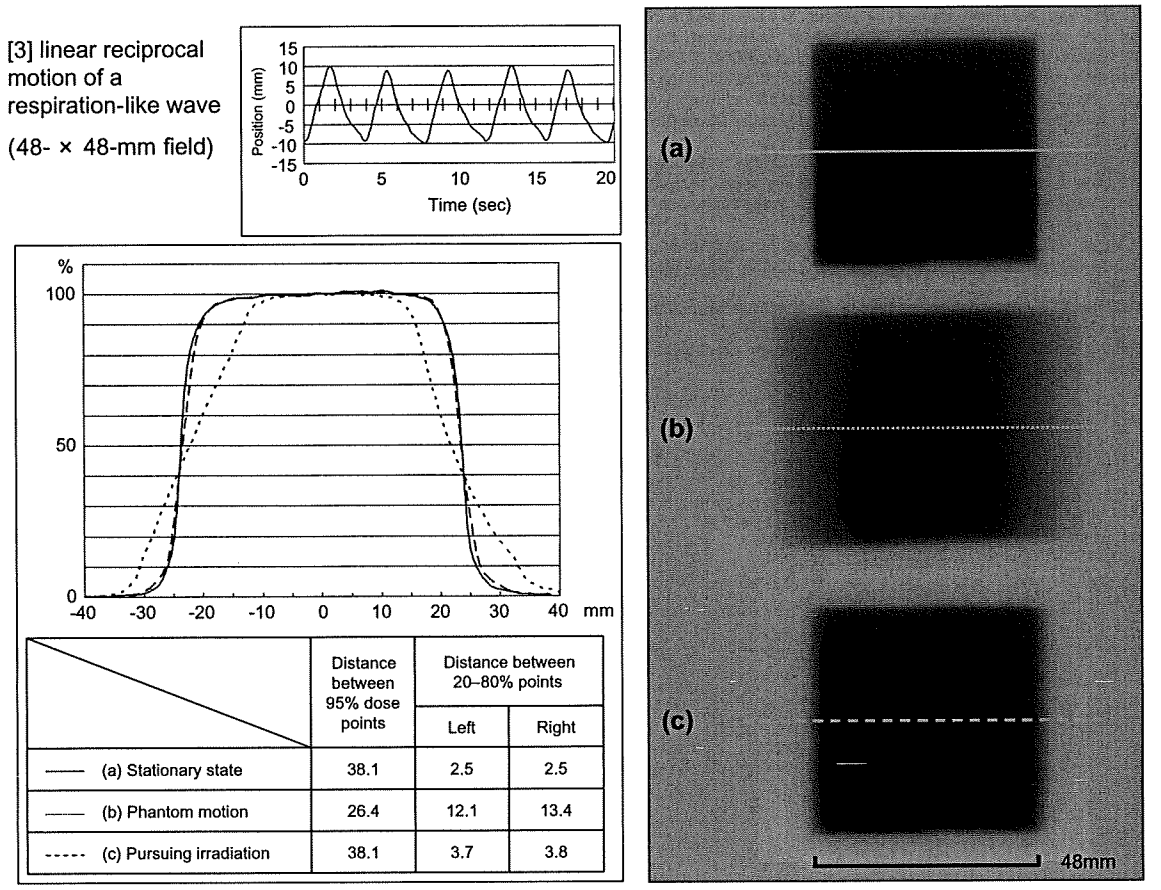

	Distance between 95% dose points	Distance between 20–80% points	
		Left	Right
—— (a) Stationary state	38.1	2.5	2.5
—— (b) Phantom motion	26.4	12.1	13.4
----- (c) Pursuing irradiation	38.1	3.7	3.8

Fig. 2. Film irradiation experiment using a 48 × 48-mm field. The line dose profiles were normalized at the field center. The effect of pursuing irradiation on motion-induced marginal blurring is visually and numerically demonstrated.

However, the sampling rate is limited by processing time, and the rate we used in this study (7.5 frames/s) is the maximum possible using the system described here. Excessively high imaging frame rates are not feasible in clinical practice because of exposure to the imaging dose.

Although a few potential problems remain to be resolved, our data indicate that this gimbals tracking system is well balanced and potentially ideal for realizing pursuing irradiation.

Conclusion

A movable phantom was used to examine the basic capabilities of a novel, gimbal-mounted IGRT system. Pursuing irradiation with this system significantly reduced motion-induced marginal blurring. Further research is underway to refine this technique for clinical use.

Conflict of interest

Kenji Takayama, Noriyuki Kawada, Hiroshi Nakayama, and Yuichiro Kamino are employees of Mitsubishi Heavy Industries and have been developing the image-guided radiation therapy (IGRT) system described here. Takashi Mizowaki, Masaki Kokubo, and Masahiro Hiraoka have a consultancy agreement with Mitsubishi Heavy Industries.

Acknowledgments

This work was partially supported by Grants-in-Aid for scientific research from the Ministry of Education, Culture, Sports, Science, and Technology (20229009) of Japan; Grants-in-Aid for Scientific Research on Priority Areas Cancer from the Ministry of Education, Culture, Sports, Science, and Technology (17016036); the Association for Nuclear Technology in Medicine; and the New Energy and Industrial Technology Development Organization (NEDO) in Japan. These study sponsors played no role in the study design, collection, analysis and interpretation of data, writing of this manuscript, or the decision to submit this manuscript for publication.

The first author gratefully acknowledges Ayuko Yamaguchi for her editorial assistance in English, and her private and spiritual support as his affectionate wife.

This work was partially presented at the 47th Annual Meeting of American Society for Therapeutic Radiology and Oncology, October 2005, Denver, CO.

References

[1] Keall PJ, Mageras GS, Balter JM, et al. The management of respiratory motion in radiation oncology report of AAPM Task Group 76. Med Phys 2006;33:3874–900.
[2] Shirato H, Suzuki K, Sharp GC, et al. Speed and amplitude of lung tumor motion precisely detected in four-dimensional setup and in real-time tumor-tracking radiotherapy. Int J Radiat Oncol Biol Phys 2006;64:1229–36.
[3] Bortfeld T, Jiang SB, Rietzel E. Effects of motion on the total dose distribution. Semin Radiat Oncol 2004;14:4151.

[4] McCarter SD, Beckham WA. Evaluation of the validity of a convolution method for incorporating tumour movement and set-up variations into the radiotherapy treatment planning system. Phys Med Biol 2000;45:923931.
[5] Negoro Y, Nagata Y, Aoki T, et al. The effectiveness of an immobilization device in conformal radiotherapy for lung tumor: reduction of respiratory tumor movement, evaluation of the daily setup accuracy. Int J Radiat Oncol Biol Phys 2001;50:889898.
[6] Onishi H, Kuriyama K, Komiyama T, et al. A new irradiation system for lung cancer combining linear accelerator, computed tomography, patient self-breath-holding, patient-directed beam-control without respiratory monitoring devices. Int J Radiat Oncol Biol Phys 2003;56:1420.
[7] Wong JW, Sharpe MB, Jaffray DA, et al. The use of active breathing control (ABC) to reduce margin for breathing motion. Int J Radiat Oncol Biol Phys 1999;44:911919.
[8] Ohara K, Okumura T, Akisada M, et al. Irradiation synchronized with respiration gate. Int J Radiat Oncol Biol Phys 1989;17:853857.
[9] Kubo HD, Hill BC. Respiration gated radiotherapy treatment: a technical study. Phys Med Biol 1996;41:8391.
[10] Wurm RE, Gum F, Erbel S, et al. Image guided respiratory gated hypofractionated Stereotactic Body Radiation Therapy (H-SBRT) for liver, lung tumors: initial experience. Acta Oncol 2006;45:881889.
[11] Murphy MJ. Tracking moving organs in real time. Semin Radiat Oncol 2004;14:91100.
[12] Keall PJ, Joshi S, Vedam SS, et al. Four-dimensional radiotherapy planning for DMLC-based respiratory motion tracking. Med Phys 2005;32:942951.
[13] D'Souza WD, Naqvi SA, Yu CX. Real-time intra-fraction-motion tracking using the treatment couch: a feasibility study. Phys Med Biol 2005;50:4021–33.
[14] Kamino Y, Takayama K, Kokubo M, et al. Development of a four-dimensional image-guided radiotherapy system with a gimbaled X-ray head. Int J Radiat Oncol Biol Phys 2006;66:271278.
[15] Nakayama H, Mizowaki T, Narita Y, et al. Development of a three-dimensionally movable phantom system for dosimetric verifications. Med Phys 2008;35:1643–50.
[16] Durbin J. The fitting of time series models. Rev Inst Int Stat 1960;28:233–43.

臨床経験

定位放射線治療後の局所再発肺癌に対する肺葉切除

祢里真也　喜夛村次郎　小松輝也　高橋　豊
竹嶋　好　加地玲子　林　三千雄　西村尚志
富井啓介　片上信之　石原享介　小久保雅樹*

はじめに

近年，非小細胞肺癌において，定位放射線治療（stereotactic radiotherapy：SRT）が施行されており，良好な治療成績が報告されている[1]．SRTは低侵襲で局所制御率も高く，高齢者や低肺機能患者にも適応できるが，照射後に局所再発をきたした症例の治療方針は一定の見解が得られていない．今回，SRT後の局所再発に対し，根治的外科切除を施行したので報告する．

I．症　例

症　例　78歳，男．

主　訴：胸部異常影．

既往歴：結腸癌（polypectomy）．

現病歴：2000年，大腸ポリープにてpolypectomy後（管状腺癌），経過観察されていた．2006年7月，PET-CTで左肺尖部にFDG異常集積を伴う5×10 mm大の腫瘍を認めたため，当院呼吸器内科を受診した．CTガイド下生検で左上葉肺扁平上皮癌（cT1N0M0）と診断された．手術をすすめるも，本人が低侵襲の治療を希望したため，同年9月に先端医療センター放射線科でSRT 48 Gy/4 Frが施行された．同年11月の胸部CTで腫瘍は3×5 mmへ縮小し，治療効果は部分奏効（partial response：PR），有害事象としてgrade 1の皮膚炎を認めた（common terminology criteria for adverse events：CTCAE v3.0）．しかし2007年4月の胸部CTでは，腫瘍

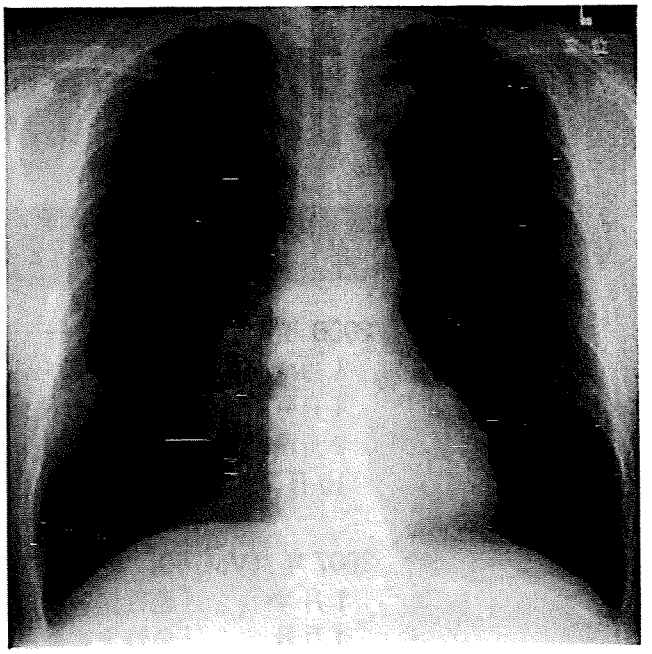

図1．当科初診時胸部X線像
左上肺野に異常影を認める．

キーワード：定位放射線治療，局所再発，非小細胞肺癌

*S. Neri, J. Kitamura, T. Komatsu, Y. Takahashi（部長）〈呼吸器外科〉, Y. Takeshima, R. Kaji, M. Hayashi（医長）, T. Nishimura（医長）, K. Tomii（医長）, N. Katakami（参事）, K. Ishihara（副院長／部長）〈呼吸器内科〉：神戸市立医療センター中央市民病院（〒650-0046 神戸市中央区港島中町4-6）：M. Kokubo（副部長）〈診療開発部〉：先端医療センター病院．

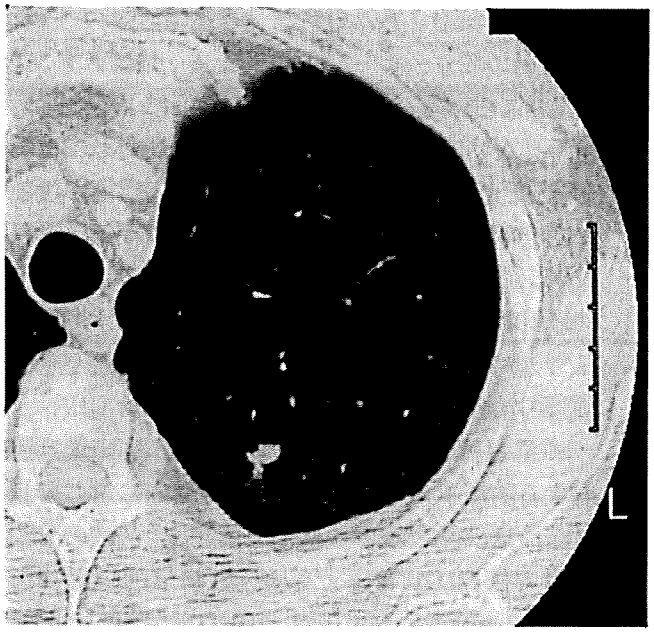

a. 呼吸器内科初診時．左 S^{1+2} に 5×10 mm 大の結節を認める．

b. SRT 施行後 2 ヵ月．腫瘍は 3×5 mm へ縮小している．

c. SRT 施行後 7 ヵ月．腫瘍は 25 mm 大に増大している．

図 2. 胸部 CT

は 25 mm 大へ増大し再燃を認めたため，同年 5 月に手術目的で当科へ紹介となった．

術前検査所見：腫瘍マーカーを含め血液検査で異常を認めなかった．呼吸機能は肺活量 2.82 *l*，%肺活量 84.2%，1 秒量 1.45 *l*，1 秒率 53.50%であり，閉塞性換気障害を認めた．

胸部 X 線所見：SRT 後 8 ヵ月の当科受診時では，左上肺野に結節影がみられた（図 1）．

胸部 CT 所見：呼吸器内科初診時には，左 S^{1+2} に 5×10 mm 大の結節を認めた（図 2a）．SRT 後 2 ヵ月で腫瘍は 3×5 mm へ縮小したが（図 2b），SRT 後 7 ヵ月で腫瘍は 25 mm 大に増大し，再燃と考えられた（図 2c）．

手術所見：2007 年 6 月，胸腔鏡補助下に左肺

上葉切除術を施行した．胸膜直下に腫瘍を認めたが，癒着はみられなかった．血管処理および気管支処理なども問題なく行えた（図3）．

病理所見：32×26×24 mmの中分化型扁平上皮癌であり，pT2N0M0と診断された．SRT施行前の生検組織と比べ，組織学的な変化はみられなかった．腫瘍再燃のため放射線照射による線維瘢痕組織なども認めなかった（図4）．

術後経過：術後7日目に呼吸不全などの合併症なく退院した．2008年8月現在，無再発で外来通院中である．

図3．手術所見
胸膜直下に腫瘍を認めるが（矢印），癒着はみられない．

Ⅱ．考　　察

肺癌診療ガイドライン2005年版によると，耐術可能な臨床病期Ⅰ期非小細胞肺癌に対しては葉切除を行うよう強くすすめている[2]．手術が可能であれば年齢の制限はなく，外科治療が第一選択と考えられている．手術ができない場合は，根治的放射線治療の適応があり，行うようすすめている[2]．本例では1秒率の低下を認め，本人が手術以外の治療を望んだためSRTを施行した．

SRTは線量集中性を高めて，より高線量を照射する治療であり，Ⅰ期非小細胞肺癌に対して良好な治療成績が報告されている[1,3,4]．従来の分割照射方法60 Gy/30 Frでは，生物学的等価線量（biological effective dose：BED）が72 Gyである一方，今回施行したSRT（48 Gy/4 Fr）のBEDは106 Gyであり，効果が高いとされている[5,6]．切除可能なⅠ期非小細胞肺癌でBED≧100 GyのSRTを施行した群において，5年生存率は臨床病期IA期で72.3%，IB期で65.9%と，手術群と比較して遜色のない成績が示されている[1]．

また，SRT施行例の14.0%に局所再発がみられ[1]，その際はすみやかに次の治療へ移行する必要がある．しかし，CTでは治療後の瘢痕組織の陰影と再発・再燃病変との区別が困難な場合が多い．FDG-PETでも，放射線肺臓炎および再発・再燃病変はともにFDG集積がみられ，鑑別がむ

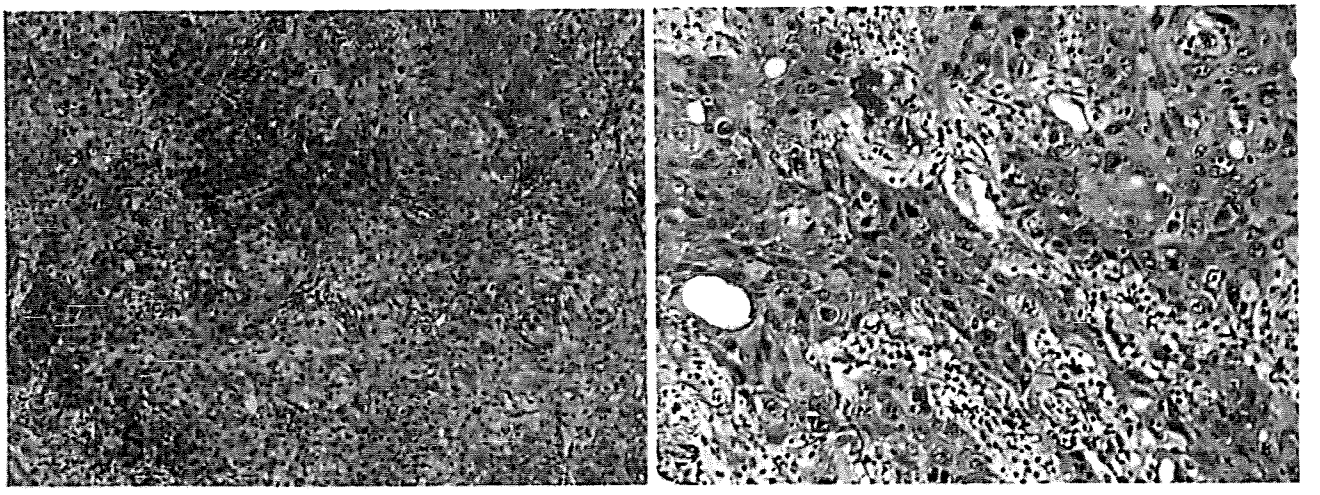

a．中拡大像　　b．強拡大像

図4．病理組織像（手術標本）［HE染色］
核の腫大と多形，分裂像が目立つ中分化型扁平上皮癌である．

ずかしい場合がある．迅速に治療を開始できるようにするには，画像や腫瘍マーカーなどの検査を頻回に行い，可能であれば生検で組織学的診断をつけることも考慮すべきである．

放射線治療後に手術を行う場合，血管・気管支周囲結合織の線維化により，胸膜や脈管の剝離に難渋することが多い．しかし，本例でのSRT後の局所再発・再然に対する外科的切除は，手術操作が困難になるほどの癒着や線維化を認めなかった．SRTは原発巣に限局した照射のため，周囲組織の癒着が起こりにくいということが示唆された．

以上より，末梢型I期非小細胞肺癌に対する治療として，はじめにSRTを施行し，局所再発・再燃例には手術を施行するという方策も考えられ，さらに症例を重ねて検討を行う必要があると思われた．

おわりに

SRT後の局所再発に対して，根治的手術を施行したので報告した．

文　献

1）Onishi H, Shirato H, Nagata Y et al : Hypofractionated stereotactic radiotherapy (HypoFXSRT) for stage I non-small cell lung cancer : updated results of 257 patients in a Japanese multi-institutional study. J Thorac Oncol 2 : S94-S100, 2007

2）日本肺癌学会（編）：非小細胞肺癌 stage I 期. EBMの手法による肺癌診療ガイドライン2005年版，金原出版，東京，p124-128, 2005

3）Nagata Y, Takayama K, Matsuo Y et al : Clinical outcomes of a phase I/II study of 48 Gy of stereotactic body radiotherapy in 4 fractions for primary lung cancer using a stereotactic body frame. Int J Radiat Oncol Biol Phys 63 : 1427-1431, 2005

4）Uematsu M, Shioda A, Tahara K et al : Focal, high dose, and fractionated modified stereotactic radiation therapy for lung carcinoma patients : a preliminary experience. Cancer 82 : 1062-1070, 1998

5）Yaes RJ, Patel P, Maruyama Y : On using the linear-quadratic model in daily clinical practice. Int J Radiat Oncol Biol Phys 20 : 1353-1362, 1991

6）Mehta M, Scrimger R, Mackie R et al : A new approach to dose escalation in non-small-cell lung cancer. Int J Radiat Oncol Biol Phys 49 : 23-33, 2001

SUMMARY

Lobectomy for Local Recurrence Following Stereotactic Radiotherapy to Non-small Cell Lung Cancer

Shinya Neri et al., Department of Thoracic Surgery, Kobe City Medical Center General Hospital, Kobe, Japan

A 78-year-old man had non-small cell lung cancer (NSCLC) in the left upper lobe (squamous cell carcinoma, cT1N0M0). He preferred less invasive treatment and undertook stereotactic radiotherapy (SRT)[48 Gy/4 Fr] because his forced expiratory volume in 1 second percent ($FEV_{1.0}$%) was 53.50%. The therapeutic effect was partial response and the adverse reaction was dermatitis (grade 1). Seven months after SRT, local recurrence was detected. The tumor was growing from 3×5 mm to 25×25 mm in size. Nine months after SRT, left upper lobectomy was performed successfully unaffected by SRT. He is doing well 14 months after the operation without any signs of recurrence. This case might help develop a new strategy for the treatment of stage I NSCLC. It is that patients with stage I NSCLC have SRT as 1st line treatment, and if local recurrence is observed after SRT, lobectomy may be performed.

KEY WORDS

stereotactic radiotherapy/local recurrence/NSCLC